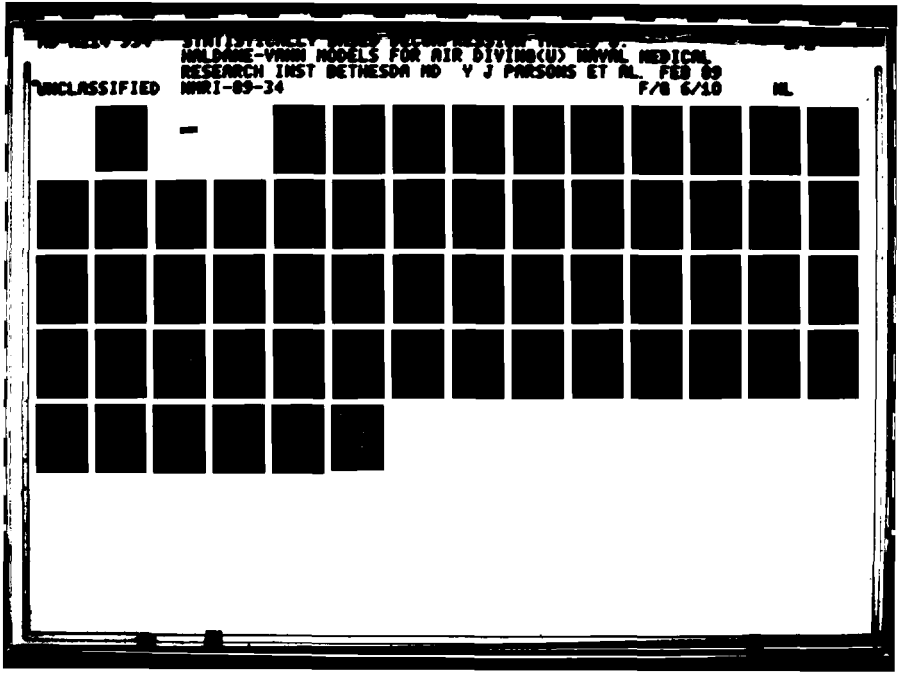
HALDANE-VANN MODELS FOR AIR DIVING(U) NAVAL MEDICAL
RESEARCH INST BETHESDA MD Y J PARSONS ET AL. FEB 89
UNCLASSIFIED NMRI-89-34 F/G 6/10 NL

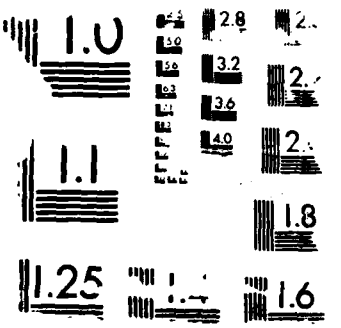
1.0
1.1
1.25
2.8
3.2
3.6
4.0
1.8
1.6

UNCLASSIFIED

SECURITY CLASSIFICATION OF THIS PAGE

REPORT DOCUMENTATION PAGE

1a. REPORT SECURITY CLASSIFICATION UNCLASSIFIED	1b. RESTRICTIVE MARKINGS
2a. SECURITY CLASSIFICATION AUTHORITY	3. DISTRIBUTION / AVAILABILITY OF REPORT Approved for public release; distribution is unlimited
2b. DECLASSIFICATION / DOWNGRADING SCHEDULE	
4. PERFORMING ORGANIZATION REPORT NUMBER(S) NMRI- 89-34	5. MONITORING ORGANIZATION REPORT NUMBER(S)
6a. NAME OF PERFORMING ORGANIZATION Naval Medical Research Institute 6b. OFFICE SYMBOL (If applicable)	7a. NAME OF MONITORING ORGANIZATION Naval Medical Command
6c. ADDRESS (City, State, and ZIP Code) Bethesda, Maryland 20814-5055	7b. ADDRESS (City, State, and ZIP Code) Department of the Navy Washington, DC 20372-5120
8a. NAME OF FUNDING / SPONSORING ORGANIZATION Naval Medical Research & Development Command 8b. OFFICE SYMBOL (If applicable)	9. PROCUREMENT INSTRUMENT IDENTIFICATION NUMBER
8c. ADDRESS (City, State, and ZIP Code) Bethesda, Maryland 20814-5044	10. SOURCE OF FUNDING NUMBERS PROGRAM ELEMENT NO. 63713N; PROJECT NO. M0099; TASK NO. 01A; WORK UNIT ACCESSION NO. DN177792

11. TITLE (Include Security Classification)

(U) STATISTICALLY BASED DECOMPRESSION TABLES V: HALDANE-VANN MODELS FOR AIR DIVING

12. PERSONAL AUTHOR(S)

Parsons, Y.J., P.K. Weathersby*, S.S. Survanshi, and E.T. Flynn

13a. TYPE OF REPORT	13b. TIME COVERED	14. DATE OF REPORT (Year, Month, Day)	15. PAGE COUNT
Final	FROM 1/87 TO 11/88	February 1989	62

16. SUPPLEMENTARY NOTATION

*Naval Submarine Medical Research Laboratory, Groton, CT 06349

17. COSATI CODES			18. SUBJECT TERMS (Continue on reverse if necessary and identify by block number)
FIELD	GROUP	SUB-GROUP	Decompression sickness; mathematical models; inert gas kinetics; risk assessment; (RT)

19. ABSTRACT (Continue on reverse if necessary and identify by block number)

This report continues the analysis of air decompression diving by probabilistic models evaluated using the statistical tool of maximum likelihood. Models based on the traditional deterministic calculations of Haldane have been placed in a probabilistic formalism by Vann. The ability of these models to fit data examined in the first and fourth reports in the present series were explored here. The computationally simpler Haldane-Vann (H-V) models achieved comparable success fitting relatively homogeneous data to the risk models used in the earlier reports in this series. However, H-V models were unable to deal successfully with larger and more diverse collections of data. It appears that the Vann definition of decompression "dose" intrinsically cannot lead to simultaneously successful predictions of both short and long air dives.

20. DISTRIBUTION / AVAILABILITY OF ABSTRACT	21. ABSTRACT SECURITY CLASSIFICATION
☒ UNCLASSIFIED/UNLIMITED ☐ SAME AS RPT ☐ OTIC USERS	Unclassified
22a. NAME OF RESPONSIBLE INDIVIDUAL REGINA HUNT, Command Editor	22b. TELEPHONE (Include Area Code) (202) 295-0198
	22c. OFFICE SYMBOL ISD/ADMIN/NMRI

DD FORM 1473, 84 MAR 83 APR edition may be used until exhausted. All other editions are obsolete.

SECURITY CLASSIFICATION OF THIS PAGE

UNCLASSIFIED

ACKNOWLEDGEMENTS

This study was funded by the Naval Medical Research and Development Command Work Unit No. M0099.01A-1002. The opinions and assertions contained herein are the private ones of the authors and are not to be construed as official or reflecting the view of the United States Navy or the Naval Service at large.

The authors are very grateful to Dr. R.D. Vann for providing pre-prints and other details of his work; to many of our colleagues, especially Dr. G. Albin for applying the risk models to the air saturation data, and Dr. L.D. Homer for stimulating discussions and suggestions; and to Ms. S. Cecire and Ms. J. Gaines for their editorial assistance.

TABLE OF CONTENTS

LIST OF TABLES

Page

LIST OF FIGURES

LIST OF APPENDICES

I. BACKGROUND

This report continues a series of studies aimed at predicting the probability of a man suffering from decompression sickness, P(DCS), following a hyperbaric exposure. The studies are based on the non-traditional assertion that DCS is not perfectly predetermined, but rather that each case is a random event having a calculable probability that applies to all men undergoing the same exposure (1). In the first report of the series (2; referred to as Report I throughout the text), a family of empirical mathematical models was developed and statistically compared to the known outcome of over 1700 well described air dives from 3 countries over a period of 20 years. Several of these models showed a powerful ability to match the known frequency of DCS in dives that ranged from 40-625 feet of seawater (fsw) in depth and 0.3-360 min in duration. The second report (3; referred to as Report II throughout the text) then took the most successful model and calculated time-optimized air decompression schedules having target incidences of 1% and 5% DCS. The third report (4; referred to as Report III throughout the text) compared the expected P(DCS) for current U.S. Navy, Royal Navy, and Canadian Forces decompression tables. In the fourth report (5; referred to as Report IV throughout the text) another 279 dives were examined in which the divers began in a saturated condition at depth (over 40 h exposure) before beginning decompression on air or other N_2-O_2 gas mixtures. Models were extended to cover both those long dives as well as the previously studied dives, and several sets of optimized saturation decompression tables calculated using one of the models.

The model evaluation process in Reports I and IV (2,5) was lengthy and computer intensive. Most details of those reports will not be repeated here; the reader will need to consult those references if additional details are

needed. In a more recent development, Vann applied a model to the problem whose computationally simpler form was appealing (6). Vann reported substantial success using Haldane's approach (7) in a probabilistic equation, although he reported difficulty in simultaneously fitting different types of exposures. After consultation with Vann, we realized that his data were not identical to those used in Reports I and IV (2,5), so that direct comparison of the success in fitting data among the different models with those reports was impossible. Furthermore, he used a parameter estimation procedure - a decreasing step size grid search - which has unknown convergence properties and fails to provide many of the statistical measures we have found important in most estimation problems.

This report explores the ability of the Haldane-Vann (H-V) approach to fit the identical data previously examined in Reports I-IV with integral risk models. In that exploration, several features of traditional decompression formulae (e.g., how many multiple parallel compartments are necessary?) were examined for statistical support from the available data. Overall, it appears that both approaches are fruitful for relatively small and homogeneous data, but that the H-V approach is rather poor at describing larger more extensive sets of dives.

II. DATA SOURCES

The data in Table 1 have been described in Reports I and IV (2,5). Individual data sets were selected to be reasonably homogeneous collections of depth-time combinations reported as a single study. Within a set, we expect only unimportant differences in subject population, diving procedures, and DCS diagnostic criteria. Set L is an exception to that rule, as it required assembly from many different sources. It is part of the data introduced in

Report IV (5) as saturation dives, and only those breathing air throughout were selected for use here. Both sets D and L have some dives with the outcome described originally as a set of symptoms apparently related to the dive but not treated as DCS. These marginal cases are assigned an outcome of 0.5 as in previous analyses (1,8). Data summary is presented below.

TABLE 1

DECOMPRESSION DATA SETS

Data Set	DCS	Dives	%DCS	Type Exposure	Reference
A	27	568	4.8	U.S. Standard Air Dive Trials, 1957	Des Grange, 1956 (9)
B	21	46	45.7	U.S. Exceptional Air Dive Trials, 1957 (all 140 fsw for 90-360 min)	Workman, 1957 (10)
C	4	299	1.3	U.K. Submarine escape trials	Donald, 1970 (11)
D	24	800	3.0	DCIEM Chamber Dives, 1967-8	Weathersby, 1985a and Tikusis et al., 1988 (2,12)
L	24.5	122	20.1	Air Saturation Dives	Hays et al., 1986 (5)

Data was encoded to list all pressure-time node points and presume a linear ramp of pressure between nodes. We note that Vann used some of the data from Sets A and B, but assumed instantaneous ascent between depths (6).

III. MATHEMATICAL MODELS

All candidate models must express P(DCS) as a function of the detailed time-pressure history of each dive profile. Reports I-IV (2-5) used a risk model:

$$P(DCS) = 1.0 - \exp\left(-\int r\, dt\right) \qquad [1]$$

In Eqn. [1] r is one of a family of instantaneous "risks" dependent on a calculated tissue nitrogen partial pressure and the current ambient pressure. A short summary of risk models is found in Appendix A of this report. The integration of Eqn. [1] was performed over the duration of the decompression and 12 hours following arrival back at 1 ATA (24 hours after saturation dives). Although performed analytically, the integration involved significant computation for the complex dive profiles.

Gas kinetic calculations are performed in all decompression methods. In the approach of Haldane, theorists have considered a handful of "tissue compartments" having exponential washout kinetics or solute residence times (referring to the parallel exponential calculations and identified by the exponential half-times, but never identified with any anatomic tissue in a real organism). The calculated tissue nitrogen partial pressure in each tissue immediately before decompression is divided by the ambient pressure immediately after decompression to obtain a "supersaturation ratio." By Haldane's original method, this ratio was declared to be a critical 1.60 at

the boundary between safe (lower ratio) and unsafe (higher ratio) decompression steps.[1] In the 80 years since Haldane, subsequent workers have developed more complex rules. Instead of a single ratio rule, newer schemes have up to many dozens of critical ratios (CR), with different rules for different tissues and different depths. No statistical analysis was ever performed to ask how many tissues and how many CR are justified by data.

Vann (6) has begun such an analysis by first defining a decompression dose, D, as the maximum "excess" supersaturation ratio at any time in any tissue, DR:

$$D = \max\{DRi(t) : 1 \leq i \leq NT,\ t > 0\} \qquad [2]$$

$$DRi(t) = (PTi(t)/PA(t)) - CRi \qquad [3]$$

where NT is the number of different "tissues" or time constants, and where PTi(t)/PA(t) is referred to as supersaturation ratio.

PTi(t) = tissue pressure at time t in tissue i calculated under the assumption of monoexponential tissue residence time distribution function (rtf), as in Report I, p. 42 (2)

PA(t) = ambient pressure

CRi = critical ratio for tissue i; CRi>1.0

For each tissue, the maximum DR at each ramp is calculated, then maximum DR over any time in the dive (over all ramps) is decided. The dose, D, is therefore defined as the single maximum of DR over all tissues for the entire dive. Vann then used the following Hill equation for decompression dose

---

[1]Haldane expressed the ratio of 2.0 as air pressure, of which only about 80% is inert gas (7).

response instead of the risk model given in Eqn. [1]:

$$P(DCS) = D^n/(D^n + D50^n) = 1/[1+ (D50/D)^n)] \qquad [4]$$

In the Hill equation, n and D50 are positive empirical parameters with no physiological interpretation. Parameter D50 is the maximum excess supersaturation that will cause a 50% incidence of DCS. The power parameter n controls the sharpness of the dose-response curve near D50 (higher values of n make the curve steeper). Other estimated parameters are the time constant (or half-time) and the CR for each tissue.

In addition to the specific models of Vann, we also examined the possible dependence of CR on ambient pressure. For that purpose, a more general definition of the critical ratio was explored:

$$CRi(t) = \max\{1.0, Ci-SCRi \cdot PA(t)\} \qquad [5]$$

Here both critical ratio intercept Ci and the critical ratio slope SCRi are positive parameters. When SCRi is fixed at 0, CRi(t) is constant and equivalent to CRi in Eqn. [3]. For positive values of SCRi, CRi will be smaller at deeper depths than at shallower depths. Also, whenever the dose defined above is negative, it is set at zero to avoid negative risks of DCS. Additional mathematical details of the models are provided under ANALYTICAL PROCEDURE and in APPENDIX B.

The H-V approach was incorporated into ten specific models in addition to the null model. The "Null model," which ignores all effects of depth and time and uses a constant P(DCS) for each dive. Its usefulness is as a lower bound on the likelihood function for comparison to more interesting models. The

likelihood function or its commonly used natural logarithm ("log likelihood" or LL) is our single most reliable measure of how well a model fits the data (1,2,13).

The models, in summary, are as follows:

MODEL 0 (NULL MODEL), P(DCS) = Total DCS / Total Dives = constant irrespective of different compression and decompression procedures among the dives.

The H-V models are categorized according to the number of tissues (NT) each with its own time constant, whether the POWER n in Eqn [4] is estimated, and whether the critical ratio CR is constant or depth-dependent, Eqn [5]. Each model must also estimate the 50% dose, D50, and 1 or more time constants.

MODEL 1, NT=1, POWER=1, constant CR

3 parameters: D50, time constant, constant critical ratio

MODEL 2, NT=1, constant CR

4 parameters: POWER, D50, time constant, constant critical ratio

MODEL 3, NT=2, POWER=1, constant CR

5 parameters: D50, 2 time constants, 2 constant critical ratios

MODEL 4, NT=2, constant CR

6 parameters: POWER, D50, 2 time constants, 2 constant critical ratios

MODEL 5, NT=3, POWER=1, constant CR

7 parameters: D50, 3 time constants, 3 constant critical ratios

MODEL 6, NT=3, constant CR

8 parameters: POWER, D50, 3 time constants, 3 constant critical ratios

MODEL Q1, NT=1, POWER=1, depth-dependent critical ratio,

4 parameters: D50, time constant, critical ratio, ratio slope

MODEL Q2, NT=1, depth-dependent critical ratios

5 parameters: POWER, D50, time constant, critical ratio, ratio slope

MODEL Q3, NT=2, POWER=1, depth-dependent critical ratio

7 parameters: D50, 2 time constants, 2 critical ratios, 2 ratio slopes

MODEL Q4, NT=2, depth dependent critical ratio

8 parameters: POWER, D50, 2 time constants, 2 critical ratios, 2 ratio slopes

IV. ANALYTICAL PROCEDURE

Fitting of models to data used the modified Marquardt (14) non-linear estimation algorithm as done previously (15). For each dive profile, the depth-time history was followed to obtain a current estimate of P(DCS) or P(no DCS), which is = 1.0 - P(DCS), depending on whether the dive resulted in DCS or not. The natural log of each P was summed over all dives to obtain the log likelihood value (LL in RESULTS tables). Parameters of the model were adjusted by the Marquardt algorithm (14) to increase LL until it achieved an apparent maximum. In general, we used several different sets of starting parameters to ensure an actual maximum. When it had been achieved, approximate uncertainties in the parameters and correlations among them were calculated by standard methods using the inverted matrix of partial derivatives of LL with respect to all parameters (13).

The best model for each data set can be decided by the Likelihood Ratio (LR) test. Two similar models, one more general than the other, can be compared for goodness-of-fit using the LR test (1,13). Specifically, the test asks whether the improvement in LL achieved by additional parameters was greater than might be expected by chance (Conceptually, the process is similar

to asking whether the fit of a straight line is significantly improved by fitting a quadratic curve or whether the apparently better fit with the additional parameter is due to chance alone). For an improved fit at $p<.05$, about 1.94 greater LL is required per additional parameter. Present statistical theory does not allow rigorous comparisons among the LL of models that cannot be expressed in simpler forms of one another. Therefore, values of LL for dissimilar models (e.g., H-V models to earlier risk model) were compared only informally.

Although we expected the present models to be computationally simpler than those of Reports I-IV (2-5), there were non-trivial analytical problems. The first follows from the definition of dose as a maximum DR over time and tissues in Eqn. [2]. We proved that for a constant critical ratio the maximum DR during any given pressure ramp would occur at the starting or end node of that ramp. For the variable depth CR in Eqn. [5], other possibilities must be considered (Appendix B).

Another class of problems arose from the discontinuous nature of the models. Discontinuities occur because of the choice of a maximum and because of the rejection of negative DR's (see equation [3]). The discontinuities produce regions of parameter space where the local gradients of LL with respect to the parameters are zero. Since our algorithm, like most nonlinear searches, uses local gradient information, there are parameter values that will not allow the maximum likelihood to be found. It was necessary to use artificially continuous formulations, and numerous starting parameter values (including some values obtained from grid searches) to convince ourselves that a global maximum likelihood was actually achieved.

The operation of these models are illustrated in Figs. 1 (a dive with continuous decompression) and 2 (a dive with staged decompression). In

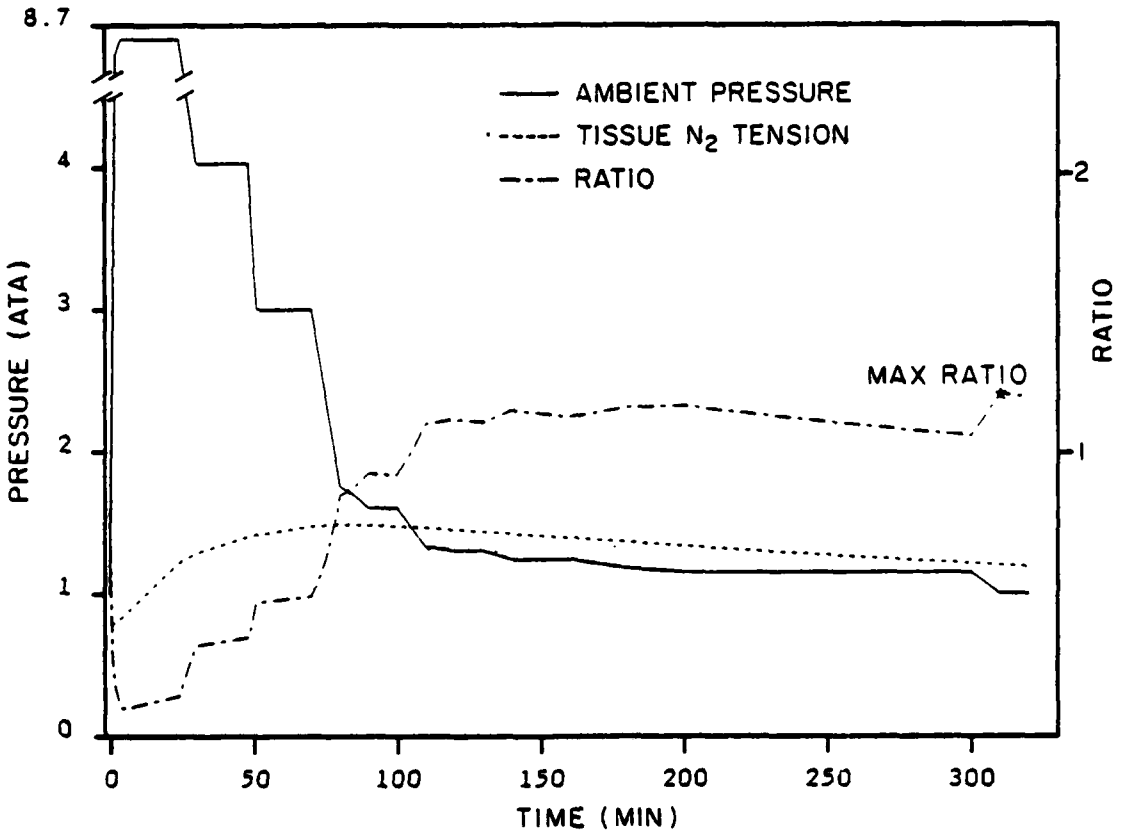

Figure 1

Supersaturation Ratio in 250/24 Trial

Time course of ambient pressure, calculated tissue pressure and supersaturation ratio. This was a 250 ft (8.85 ATA), 24-minute dive. The 8 same dives produced 1 confirmed and 1 marginal case of DCS. Model 2 of Data Set D has N=1.7, D50=1.3, T=295, CR=1. Scale of ratio is twice the ATA, on the right margin.

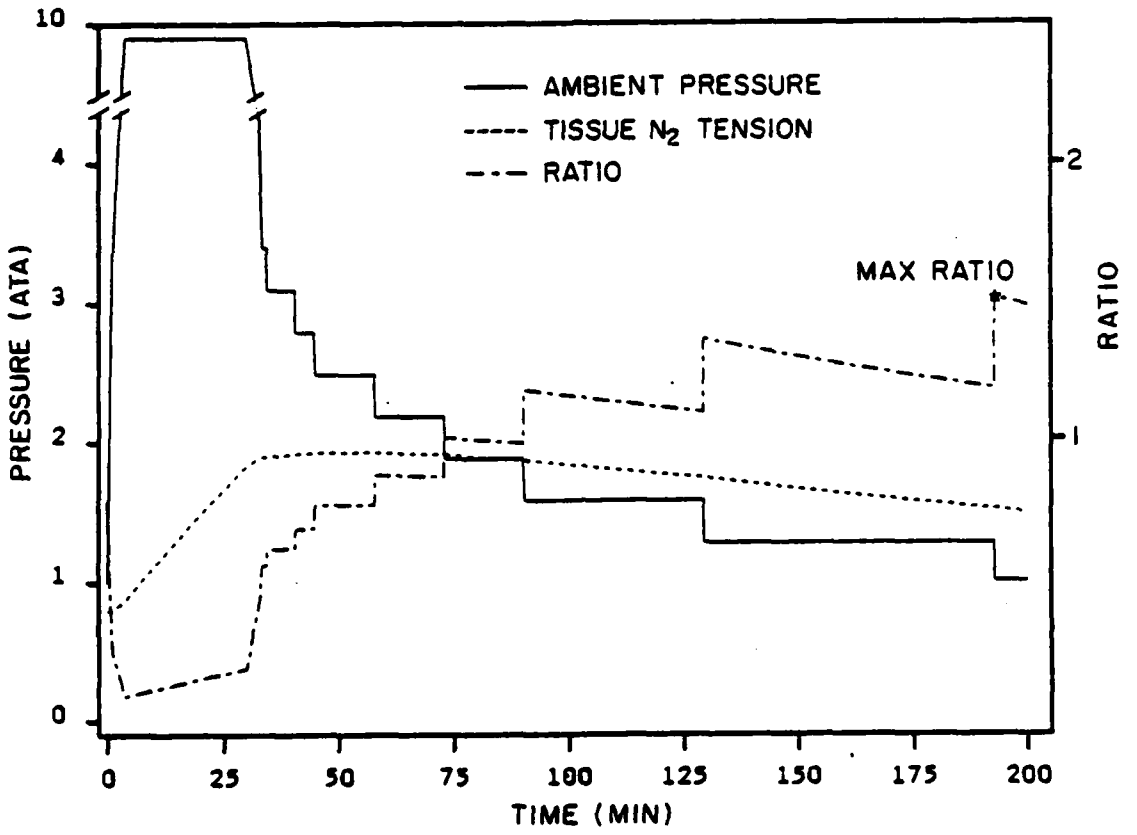

Figure 2

Supersaturation Ratio in 287/30 Trial

Time course of ambient pressure, calculated tissue pressure, and supersaturation ratio. This was a 287 ft (4 same dives produced 1 case of DCS) (9.7 ATA), 30-minute dive. Model 1 of Data Set A has N=1, D50=1.67, T=172, CR=1.3. Scale of ratio is twice the ATA on the right margin.

Fig. 1, the graph shows the depth-time profile for a dive to 250 fsw (8.58 ATA) for 24 minutes followed by a 286-min decompression procedure from Data Set D (On this dive 8 men produced 1 confirmed and 1 marginal case of DCS). The dotted line is the calculated tissue nitrogen pressure, using a time constant of 295 min from Model 2 for Set D (see Table 7). Values of the supersaturation ratio plotted as a dashed-dot line rises above 1.0 at about 80 min and has a maximum (1.202) near 310 min. The critical ratio CR is 1.000, thus leaving a maximum excess supersaturation of 0.202 as the decompression dose. With Eqn. [4], D50=1.3, and N=1.7, we calculate a P(DCS) of 4.1%. The staged decompression and tissue pressure from Model 1 for a dive from Data Set A are shown in Fig. 2. It has a jagged ratio that is in excess of the critical ratio (CR=1.3) only in a few instances. Similar calculations are repeated for every dive in the data set.

V. RESULTS and DISCUSSION

Details of parameter results are shown here for each data set and for combinations of them. In the Tables are presented final H-V parameters, with approximately 1 SE error limits, and maximum LL. Also included in each table is the best LL of risk models from Report I (models 1-6 in Report I (2) are now referred to as R1 to R6, also see APPENDIX A). The full results are not repeated here; the reader is referred to those reports for performance details of each risk model with each data set.

1. DATA SET A: STANDARD AIR DIVES (1956)

Maximum likelihood estimates are in Table 2. For these data, the simplest H-V model (Model 1) is a clear improvement over the null model (Model 0). The search for a POWER significantly different from 1.0 in the Hill dose-response function (Eqn. [4]) failed to improve the fit to data, as

TABLE 2

(DATA SET A, N = 568, BENDS = 27)

MODEL (FIXED PARAMETERS)	PARAMETERS (1 SE)			LOG LIKELIHOOD
0. CONSTANT P	P = 0.048			-108.598
1. NT = 1, POWER = 1,	D50 = 1.67 T = 172 CR = 1.3	(0.87) (84) (0.22)	*(0.78,3.4) (113,530) (1.0,1.48)	-90.312
2. NT = 1,	POWER = 0.57 D50 = 7.7 T = 156 CR = 1.36	(1.36) (69) (107) (0.24)		-90.099
3. NT = 2, POWER = 1	D50 = 0.78 T1 = 93 CR1 = 1.57 T2 = 314 CR2 = 1.25	(0.43) (12) (0.05) (603) (0.67)		-88.560
4. NT = 2,	POWER = 0.84 D50 = 1.1 T1 = 93 CR1 = 1.58 T2 = 317 CR2 = 1.26	(1.6) (4.3) (14) (0.11) (815) (0.85)		-88.426
Q1. NT = 1 POWER = 1 Variable CR	D50 = 0.89 T = 97 C1 = 1.93 SCR1 = 0.38	(0.47) (17) (0.12) (0.14)		-88.817
R1. 1-tissue, no thresh	T = 340 A = 3.1E-3	(100) (1.1E-3)		-91.450
R2. 1-tissue, thresh	T = 122 A = 16E-2 PTHR = 11.9	(50) (2.4E-2) (7.1)(fsw)		-90.891

T, T1, etc. are in units of minutes, the other parameters are dimensionless.

Approximate 1 SE error on estimated parameters are in parentheses.

* When two sets of parentheses follow a parameter, the second set is found by examining the likelihood surface away from maximum LL by 1.94 units.

seen in Model 2. Allowing two parallel tissues and separate critical ratios (Model 3) does not produce a significant improvement over 1 tissue by likelihood ratio test. Note that the two time constants in Model 3 are shorter (93 min) and longer (314 min) than the single one in Models 1 (172 min) and 2 (156 min). As in the previous work with risk models, increasing the number of time constants creates a new set of values, which is wider than the range previously found. Allowing POWER different from 1.0 with two tissues in Model 4 does not significantly improve the fit. Model Q1 is also not significantly better than the constant CR (Model 1). The depth dependence of the CR is shown in Fig. 3. The maximum CR at 1 ATA is 1.55 and CR drops to 1.0 at 2.45 ATA (48 fsw). Comparison with previous Models R1 and R2 shows an equivalent likelihood that suggest both types of models are adequate for these data. All successful models achieved a LL of about -90.

Some comments are appropriate about confidence limits in the parameter estimates. Table 2 entries have approximately 1 standard error of the estimates, calculated by the statistical procedure appropriate for "well behaved problems" (13). For example, Model 1 estimates a CR of 1.30 ± 0.22. For well behaved problems, we could expect an estimated CR to be within these limits about two-thirds of the time. We would also expect that a band around the best estimate of 2(SE) to contain the estimate about 95% of the time. The conceptual and numerical difficulties encountered with H-V models (reasons described under ANALYTICAL PROCEDURES) make such an interpretation less useful than in other models, for example, 1.30-2(0.22)=0.86 as an estimated lower 95% confidence limit. However, external reasons (like the need to predict no DCS if there is no decompression) require a CR greater than 1. A better way to construct a 95% confidence limit is to fix the parameter in question at values that are progressively distant from its best estimate and calculate LL while

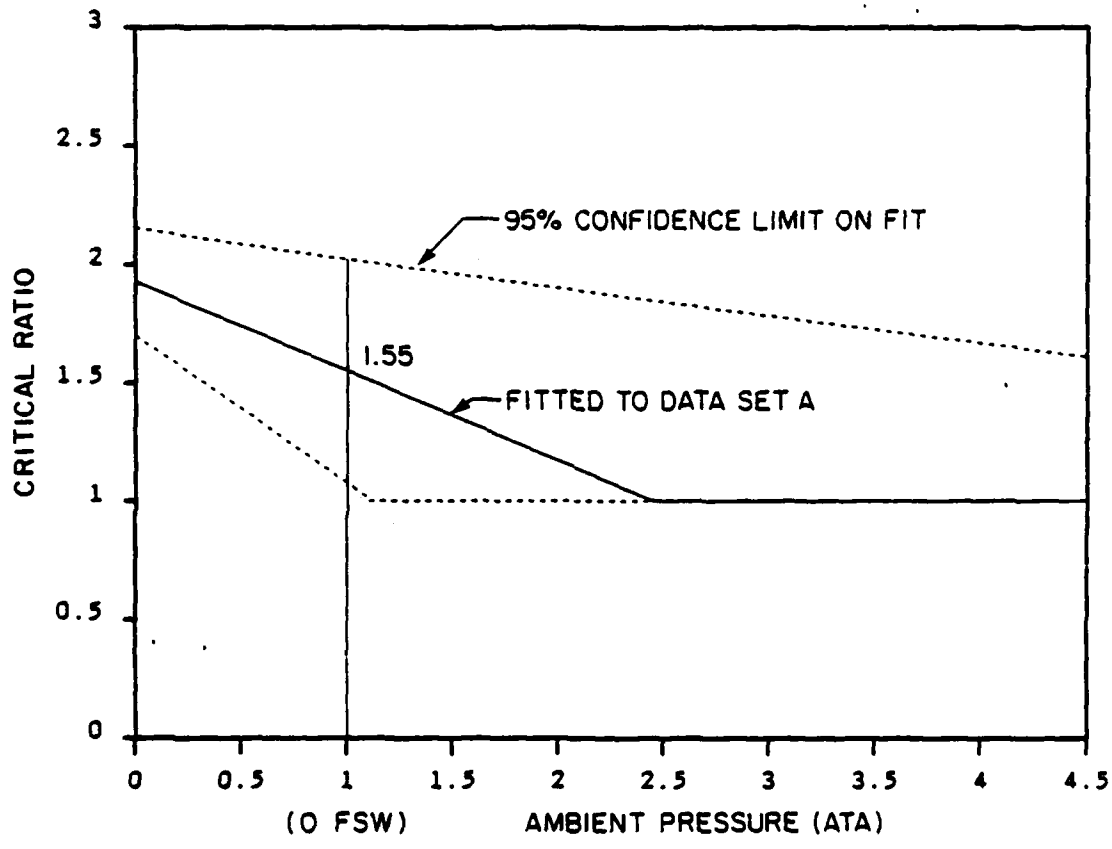

Figure 3

Depth Dependent Critical Ratio for Data Set A

Model Q1 of Data Set A has N=1, D50=0.89, T=97. C1=1.93, SCR1=0.38. Critical ratio = 1.93 - 0.38 (ambient pressure).

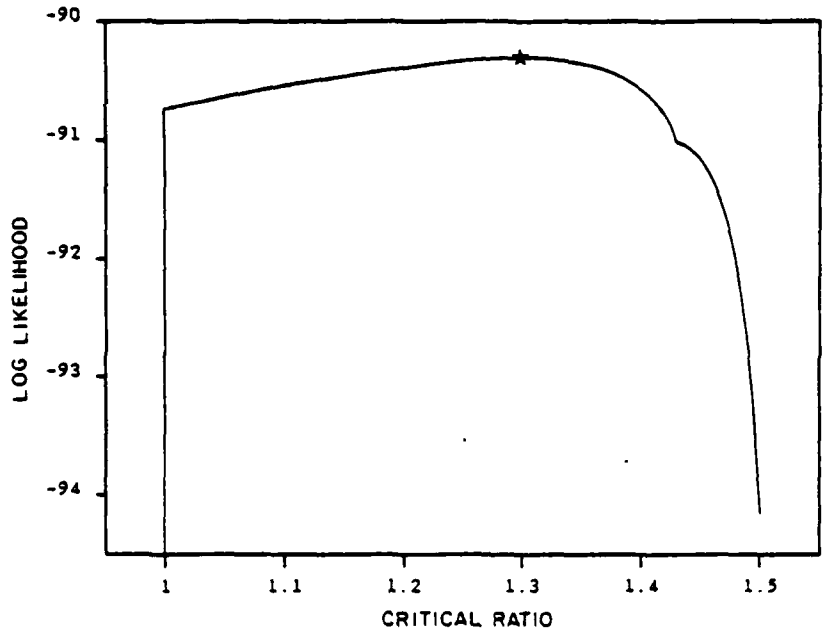

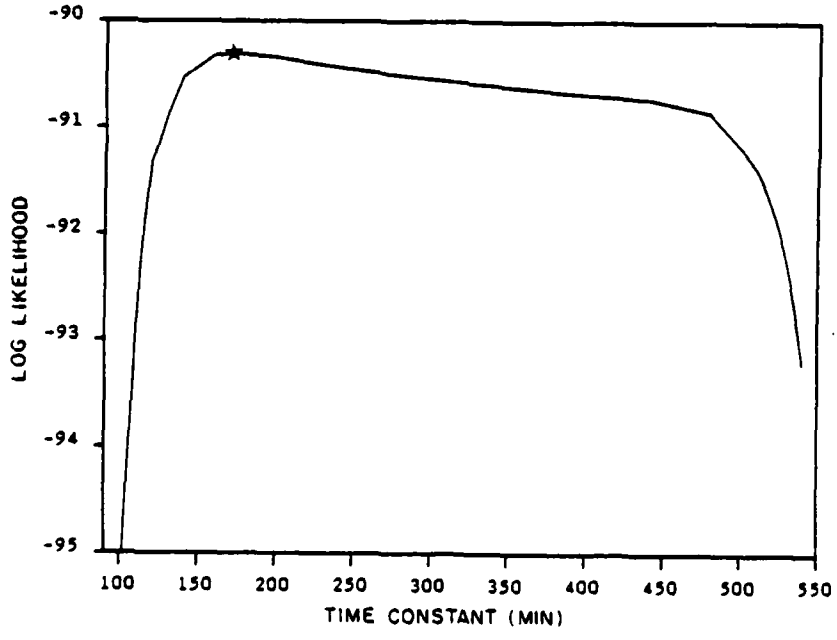

Figure 4

Likelihood of Model 1 for Data Set A

Figure 4A. Maximum LL at CR = 1.3 indicated by star

Figure 4B. Maximum LL at Time Constant = 172 indicated by star

questions such an increase in likelihood has important consequences. Vann did not report parameter values, so we cannot compare other aspects of model behavior.

In summary, the simplest H-V model was adequate for these data, as was the simplest risk model examined in Report I. Of at least historical interest is the fact that the test dives comprising Data Set A were calculated by a Haldane approach with 6 fixed time constants over a range of 5-120 min (9,16). With the time constants was a matrix of about 54 critical ratios whose value changed slightly during the testing phase itself. By the statistical evaluation reported here, models with 2-4 parameters can describe the data as well.

2. DATA SET B: EXCEPTIONAL EXPOSURE AIR DIVES (1956)

This small data set is unusually rich in DCS cases after long (2-6 h) dives. Estimation results are in Table 3. The simplest H-V model (Model 1) was a significant improvement over the null model (Model 0). The estimated time constant (347 min) is longer than for Data Set A (172 min), which is not surprising for long dives. Most of the potential models were not explored aggressively since the small data set would not support many parameters. The three-parameter risk model (Model R2) tabulated is seen to have a similar likelihood.

It should be noted that the data were obtained in an acceptance trial where the original expectation was a low incidence of DCS. When many cases occurred, the decompression times were incrementally lengthened (by ad-hoc adjustment of critical ratios), and re-tested. As soon as a seemingly lower incidence was achieved with small groups of divers (usually 6), the trial was terminated. Thus, the function of DCS incidence against decompression time (and related measures such as DR in the present model) will be artificially

TABLE 3

(DATA SET B, N = 46, BENDS = 21)

MODEL (FIXED PARAMETERS)	PARAMETERS (1 SE)		LOG LIKELIHOOD
0. CONSTANT P	P = 0.4565		-31.710
1. NT = 1, POWER = 1,	D50 = 0.065	(0.037)	-22.428
	T = 347	(17)	
	CR = 1.50	(0.02)	
2. NT = 1,	POWER = 11	(109)	-21.166
	D50 = 0.60	(5.84)	
	T = 392	(54)	
	CR = 1.00000	(5.8)	
3. NT = 2, POWER = 1			same as 1
4. NT = 2,			same as 2
R1. 1-tissue, no thresh	T = 739	(469)	-27.076
	A = 3.3E-3	(0.7E-3)	
R2. 1-tissue, thresh	T = 329	(38)	-21.680
	A = .113	(.091)	
	PTHR = 15.2	(1.5)(fsw)	

T, T1, etc. are in units of minutes, the other parameters are dimensionless.

Approximate 1 SE error limits on estimated parameters are in parentheses.

steep. The attempt to find POWER different from 1 (Model 2) produced the large and imprecise value 11 ± 109. The very large uncertainty in the POWER reflects the binomial uncertainty from the small overall size of the data. In model R2, the steep dose response surface was achieved by estimating an absolutely safe supersaturation threshold of 15 fsw. The magnitude of the POWER parameter indicates a very steep dose-response curve in the range of dives near 50% DCS, which is the range of risk seen in the raw data (overall 46% DCS). Indeed, we consistently find that none of the large data sets require a POWER nearly as large as 11 (see below). Successful fits to these data all require a LL of about -22.

3. DATA SET AB

We explored the combined Data Set AB (Set A plus Set B). Results are presented in Table 4. From earlier results, we expect good fits to the combined data to achieve a LL of about -90 (from Set A) plus -22 (from Set B) or a total of -112 LL units. All H-V models were significantly better than the null model, but none quite achieved the goal of about -112 LL units. The two-parameter risk model could not achieve the goal either. For the simplest model (Model 1), a very long time constant (503 min) was required to fit the data. This time constant is longer than those required by Data Sets A or B separately, and it required the lowest possible CR to accomplish it. The error limit on CR in Table 4 is asymmetric; the 1 SE upper bound is 1.00 ± 0.11, but the lower limit remains at 1.00 to avoid a finite risk of DCS without any tissue supersaturation (This asymmetric bound provided one of the difficult estimation problems encountered in the analysis). A model of two tissues with the power fixed at 1.0 (Model 3) did not produce a significantly improved fit over 1 tissue. However, with a power estimated at 6.1 ± 9.1 (Model 4, 6 parameters), a significantly improved maximum likelihood was

TABLE 4

(DATA SET AB, N = 614, BENDS = 48)

MODEL (FIXED PARAMETERS)	PARAMETERS (1 SE)		LOG LIKELIHOOD
0. CONSTANT p	P = 0.0782		-168.145
1. NT = 1, POWER = 1,	D50 = 0.99	(0.26)	-121.271
	T = 503	(263)	
	CR = 1.0000	(0.11)	
2. NT = 1,	POWER = 2.1	(1.5)	-119.565
	D50 = 0.66	(0.12)	
	T = 367	(129)	
	CR = 1.0000	(0.12)	
3. NT = 2, POWER = 1			same as 1
4. NT = 2,	POWER = 6.09	(9.07)	-114.858
	D50 = 0.61	(0.62)	
	T1 = 388	(61)	
	CR1 = 1.0001	(0.63)	
	T2 = 139	(14)	
	CR2 = 1.13	(0.66)	
Q1. NT = 1, POWER = 1			same as 1
Q2. NT = 1			same as 2
Q3. NT = 2, POWER = 1			same as 3
Q4. NT = 2			same as 4
R1. 1-tissue, no thresh	T = 362.3	(44)	-119.210
	A = 3.57E-3	(.63E-3)	
R2. 1-tissue, thresh	T = 318	(156)	-119.202
	A = 4.35E-3	(3.6E-3)	
	PTHR = 1.23	(4.95)(fsw)	

T, T1, etc. are in units of minutes, the other parameters are dimensionless.

Approximate 1 SE error limits on estimated parameters are in parentheses.

Expected LL for excellent fit = -112.

4. DATA SET C: SUBMARINE ESCAPE TRIALS

Data Set C is different from the other data examined because it has very short deep dives (but with only 4 cases of DCS). Fitting results are tabulated in Table 5. Again the simplest H-V model (Model 1) was a better description of the data than a null model. Allowance of a variable POWER (Model 2) did not improve the fit significantly. No other H-V models were used because the small data set would not provide enough information for the additional parameters. Model R1 had a similar likelihood. R2 is not a significant improvement over R1, but is included to show the unbelievable parameters (here a 79-fsw supersaturation as an estimated threshold) that can arise in using threshold parameters and small data sets. In all cases, the time constants were short, as expected for these short dives. About -18 LL units are associated with the better models.

5. DATA SET ABC

The 3 data sets examined so far include a wide range of diving conditions. How well do the H-V models describe the entire range? The results of fitting to combined data of sets A, B, and C are in Table 6. The simplest H-V model is actually worse than no model at all (compare LL of Model 1 with Model 0). The two-parallel tissue model, Model 3, had a substantially improved ability to fit the data. Model 4 with the low estimated POWER of 0.49 ± 0.23 is the most successful H-V model. This model required a very short time constant (0.93 min or 56 sec) with a high (4.57) critical ratio, along with a long (501 min) time constant, allowing virtually no supersaturation (CR = 1.01). None of the more complex H-V models were a better fit to the data. As with the H-V Models, the very simplest risk models did not fit the combined data (see Report I for details). Other risk models were considerably more successful than H-V in fitting the data, as seen by a

TABLE 5

(DATA SET C, N = 299, BENDS = 4)

MODEL (FIXED PARAMETERS)	PARAMETERS (1 SE)		LOG LIKELIHOOD
0. CONSTANT P	P = 0.013		-21.230
1. NT = 1, POWER = 1,	D50 = 32	(77)	-17.865
	T = 1.1	(1.2)	
	CR = 3.8	(2.8)	
2. NT = 1,	POWER = 0.14	(2.8)	-16.927
	D50 = 0.5E9	(0.2E12)	
	T = 0.9	(1.6)	
	CR = 4.5	(4.5)	
3. NT = 2, POWER = 1			same as 1
4. NT = 2			same as 2
R1. 1-tissue, no thresh	T = 12.2	(20.4)	-19.225
	A = 4.8E-3	(5.9E-3)	
R2. 1-tissue, thresh	T = 1.04	(0.94)	-18.093
	A = 7.0E-2	(27.0E-2)	
	PTHR = 79	(82)(fsw)	

T, T1, etc. are in units of minutes, the other parameters are dimensionless.

Approximate 1 SE error limits on estimated parameters are in parentheses.

TABLE 6

(DATA SET ABC, N = 913, BENDS = 52)

MODEL (FIXED PARAMETERS)	PARAMETERS (1 SE)		LOG LIKELIHOOD
0. CONSTANT P	P = 0.056		-199.496
1. NT = 1, POWER = 1	D50 = 9.28	(1.64)	-211.552
	T = 31.7	(6.7)	
	CR = 1.00001	(0.06)	
2. NT = 1,	POWER = 0.13	(0.30)	-199.782
	D50 = 0.1E9	(0.6E10)	
	T = 35	(72)	
	CR = 1.00004	(0.47)	
3. NT = 2, POWER = 1	D50 = 2.15	(0.52)	-156.720
	T1 = 400	(10)	
	CR1 = 1.0000	(0.05)	
	T2 = 0.94	(0.24)	
	CR2 = 4.55	(0.29)	
4. NT = 2,	POWER = 0.49	(0.23)	-154.385
	D50 = 10	(17)	
	T1 = 501	(10)	
	CR1 = 1.01	(0.03)	
	T2 = 0.93	(0.23)	
	CR2 = 4.57	(0.58)	
5. NT = 3, POWER = 1,			same as 3
6. NT = 3,			same as 4
Q3. NT = 2, POWER = 1,			same as 3
Q4. NT = 2			same as 4
R3. 2-tissue, no thresh	TA = 0.66	(1.6)	-139.529
	AA = 6.7E-3	(19E-3)	
	TB = 365	(50)	
	AB = 3.6E-3	(6.3E-3)	
R5. 1 tissue with 2-exp rtf no thresh	T1 = 1.5	(2.3)	-139.289
	T2 = 265	(30)	
	W1 = 0.99	(0.08)	
	A = 1.18E-2	(0.57E-2)	

T, T1, etc. are in units of minutes, the other parameters are dimensionless.

Approximate 1 SE error limits on estimated parameters are in parentheses.

Expected LL for excellent fit = -130.

much better likelihood. They also had terms for both slow and fast events: Model R3 has parallel time constants of 0.66 and 365 min, while Model R5 has a single tissue residence time function (2) composed of a 1.5 min and a 265 min process.

To more quantitatively assess whether the H-V model can fit the combined data, we can examine the expected LL for excellent fits to the individual sets: -90-22-18 = -130. The best H-V fit misses this target by about 25 LL units while R3 and R5 miss by about 10 units. The difference in model performance is quite substantial.

Additional insight into the failure of the H-V models to describe combined data is seen in Fig. 5. This graph has P(DCS) from both H-V and risk models against dive number. The dives of set A are the first 568 dives, then the 46 of set B, and the final 299 are from set C. The best H-V model (Model 4) and a successful risk model (R5) are both shown. Predictions are comparable for Data Set A, but diverge for Data Sets B and C. For the hazardous set B dives (near observation 600), Model R5 predicts an average P(DCS) of 44.4% while H-V Model 4 underestimates the risk (average of 18.9%). Later in the short and deep, but rather safe, set C dives, Model 4 overestimates the risk. Some of the discrepancy seems to be caused by the dose-response function, specifically the POWER parameter estimated for combined data. The long time constant and its CR are similar for ABC as for set B alone and for AB, but the POWER is much lower for ABC because of the attempt to fit dives from set C. It appears that no single dose-response function in the H-V models can fit both the long, severe dives and the short, safe dives. However, the H-V model and risk model agree quite well using parameters estimated only from Data Set B (line 3 and 4 in Fig. 6). This shows that the H-V model can fit Set B alone satisfactorily, but seriously

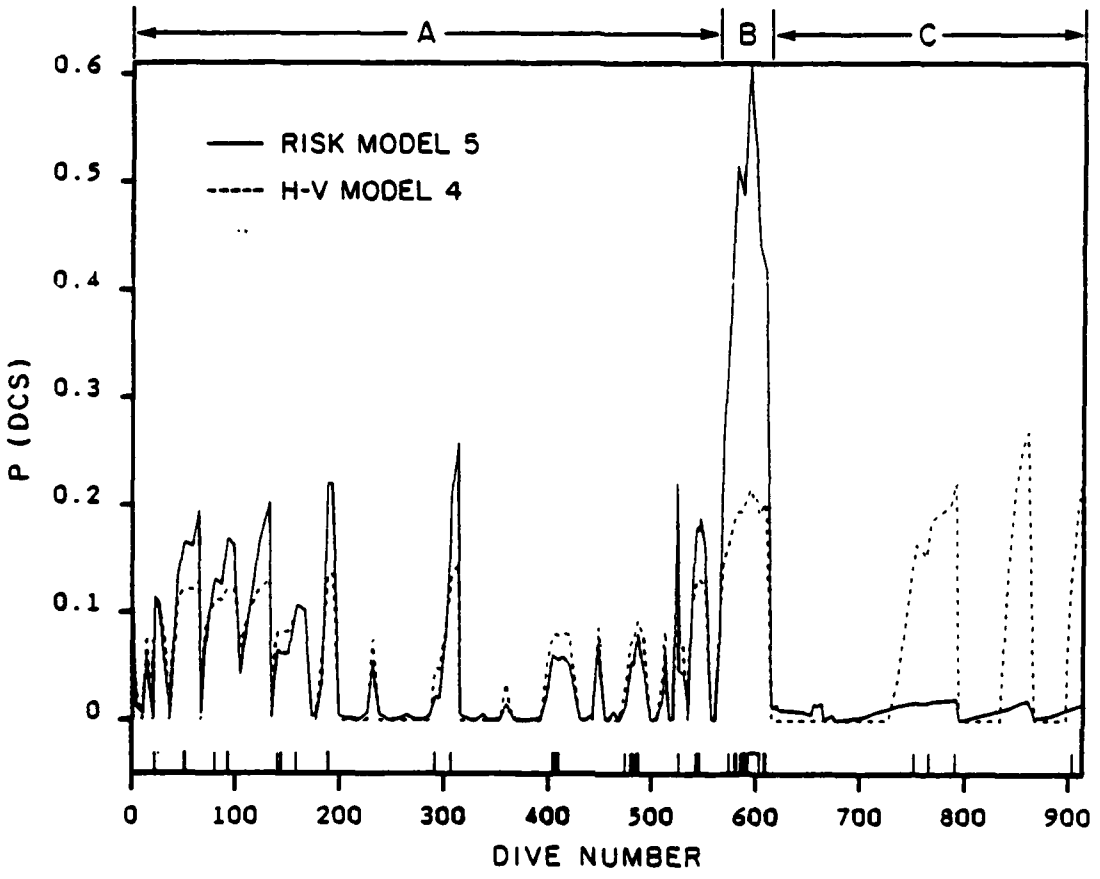

Figure 5

Comparison of Risk Model and H-V Model for Data Set ABC

Data (Dive Number)	bend%	average P(DCS) by R5	average P(DCS) by H-V4
A (1--568)	4.8%	5.2%	4.9%
B (569--614)	45.6%	44.4%	18.9%
C (615--913)	1.3%	0.9%	5.2%

*bar below 0 indicates incidence of bends

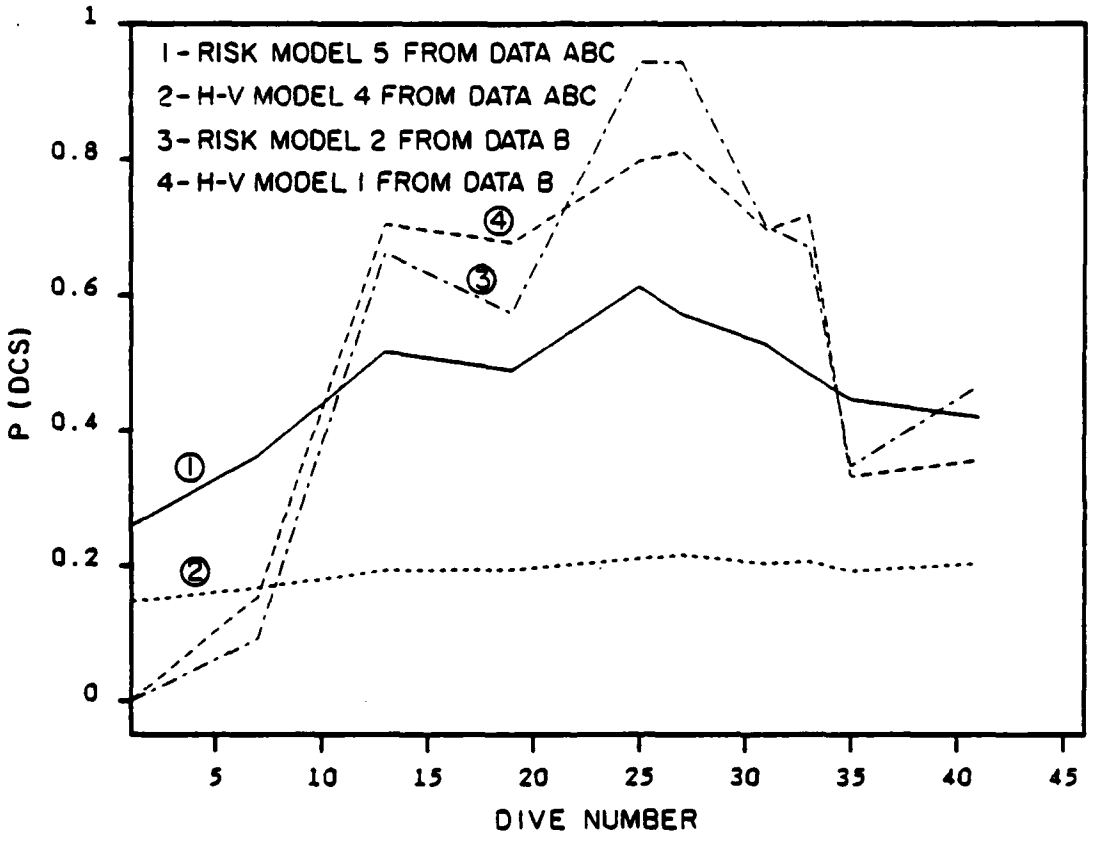

Figure 6

P(DCS) Comparison from Different Models for Data Set B

underestimates P(DCS) for Data Set B while fitting ABC. The risk model, by contrast, was able to match the higher average P(DCS) of Data Set B even while fitting the combined Data Set ABC.

6. DATA SET D: CANADIAN CHAMBER DIVES

The next data set has a mixture of depths and times (without the worry caused by combining data from different laboratories) that were recorded at various times by several investigators with diverse standards for DCS. The dives also had slow continuous decompression rates (e.g., Fig. 1A) that could test depth-dependent features of any model. The model results are in Table 7. The two single-tissue models (Models 1 and 2) are marginally significant improvements over the null model. The two-tissue models (Models 3 and 4) are real improvements. In both cases, the time constants required are about 17 and 360 min. As seen with previous data, the slower time constant has a lower CR. The risk model previously described for these data (Model R4) has a similar likelihood and parallel time constants of about 6 min and 250 min.

In another study, these same data were also well described by a model using non-monoexponential kinetics that are used to calculate decompression tables in Canada (12). The best fits by various models achieve a LL of about -95.

Unlike most of the other data, this set justifies a depth-dependent CR. Both Models Q3 and Q4 have a significantly better likelihood than their depth-independent versions, Models 3 and 4. The behaviors of the CRs are shown in Fig. 7. The longer (328 min) tissue has only a weak depth-dependence: the CR is 1.12 at the surface (1 ATA) and returns to 1.00 by 5.6 fsw (1.17 ATA). The shorter tissue (13.2 min) varies more: CR is 2.01 at the surface and does not reach 1.00 until 145 fsw (5.39 ATA). The depth-dependent functionality is possible because the data have many dives with a continuous,

TABLE 7 (Cont'd)

(DATA SET D, N = 800, BENDS = 24)

MODEL (FIXED PARAMETERS)	PARAMETERS (1 SE)		LOG LIKELIHOOD
R4. 2-tissue,	TA = 6.64	(5.4)	-97.246
	AA = 5.6E-3	(6E-3)	
	TB = 253	(107)	
	AB = 7.83E-2	(11E-2)	
	PTHR = 5.9	(5.1)(fsw)	

T, T1, etc. are in units of minutes, the other parameters are dimensionless.

Approximate 1 SE error limits on estimated parameters are in parentheses.

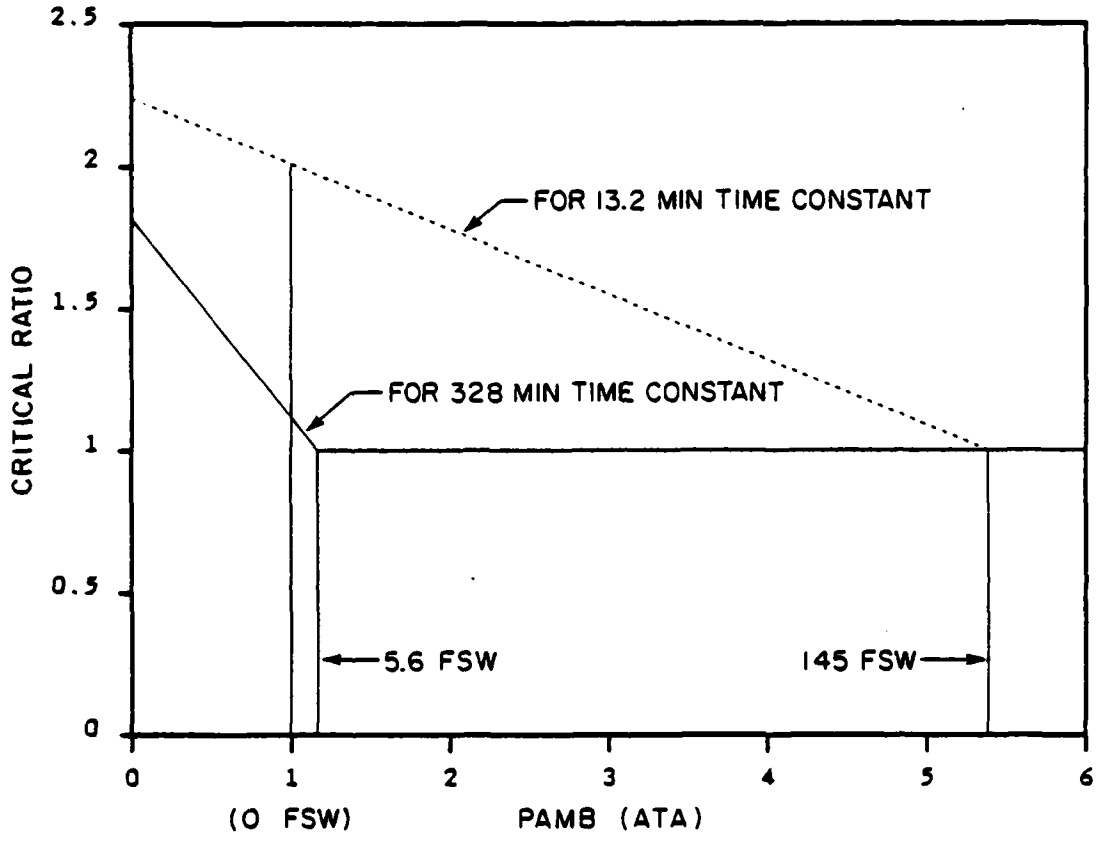

Figure 7

Depth Dependent Critical Ratio for Data Set D

Model Q3: N=1, D50=2.1, T1=328 (slow tissue), C1=1.8, SCR1=0.7,
T2=13 (fast tissue), C2=2.2, SCR2-0.22.

rather than a staged, decompression. An example of that smooth decompression is in Fig. 1, where the calculated supersaturation (ratio) is seen to change gradually (compared to the jagged ratio in Fig. 2).

7. DATA SET ABCD

Performance of the models on combined data from sets A, B, C, and D is in Table 8. Single-tissue models were not even attempted for this diverse collection of dives. The two-tissue models (Model 3 and 4) were significant improvements over the null model. Surprisingly, no three-tissue model was able to improve the likelihood over the two-tissue models. Whenever they were tried, two of the three time constants always converged to identical values as one of the time constants of the two-tissue models. Note that the five-parameter risk model is much better (a log likelihood improvement of over 20 units). The target LL for excellent fits based on individual LL is -90-22-18-95 = -225. Risk models miss that mark by about 25 units while the H-V miss by about 45 LL units.

As in Fig. 5, the failure of the H-V models to combine data is seen in Fig. 8. The best H-V (Model 4) and a successful risk model (R4) are both shown. R4 is much better than the H-V model in all 4 regions corresponding to the original data sets.

8. DATA SET ABD

As in Report I (2), we examined whether the failure to describe combined data is mostly due to inclusion of the very short exposures of Data Set C. Performance of models on combined data of sets A, B, and D (C excluded) is in Table 9. Model 2 with LL = 224.9 is the best H-V model. Risk model R4 had a better fit by 3 LL units. The exclusion of Data Set C makes the H-V models more comparable with risk models, which were still able to handle the shorter data of Set C. Therefore, short Data Set C caused much more problems for the

TABLE 8

(DATA SET ABCD, N = 1713, BENDS = 76)

MODEL (FIXED PARAMETERS)	PARAMETERS (1 SE)		LOG LIKELIHOOD
0. CONSTANT P	P = 0.04437		-311.049
1. NT = 1, POWER = 1,			NA
2. NT = 1,			NA
3. NT = 2, POWER = 1	D50 = 2.98	(0.43)	-264.230
	T1 = 0.92	(0.11)	
	CR1 = 4.52	(0.06)	
	T2 = 358	(82)	
	CR2 = 1.00000	(0.04)	
4. NT = 2,	POWER = 1.17	(0.29)	-263.743
	D50 = 2.18	(0.93)	
	T1 = 0.92	(0.10)	
	CR1 = 4.52	(0.06)	
	T2 = 347	(77)	
	CR2 = 1.00000	(0.05)	
5. NT = 3, POWER = 1			same as 3
6. NT = 3			same as 4
Q3. NT = 2, POWER = 1			same as 3
Q4. NT = 2			same as 4
R3. 2-tissue, no thresh	TA = 2.43	(1.7)	-247.085
	AA = 3.19E-3	(1.9E-3)	
	TB = 283	(44)	
	AB = 2.73E-3	(0.45E-3)	
R4. 2-tissue, thresh	TA = 6.17	(1.9)	-242.250
	AA = 3.16E-3	(1.2E-3)	
	TB = 260	(39)	
	AB = 7.63E-3	(3.0E-3)	
	PTHR = 5.03	(1.7)(fsw)	

T, T1, etc. are in units of minutes, the other parameters are dimensionless.

Approximate 1 SE error limits on estimated parameters are in parentheses.

Expected LL for excellent fit = -225.

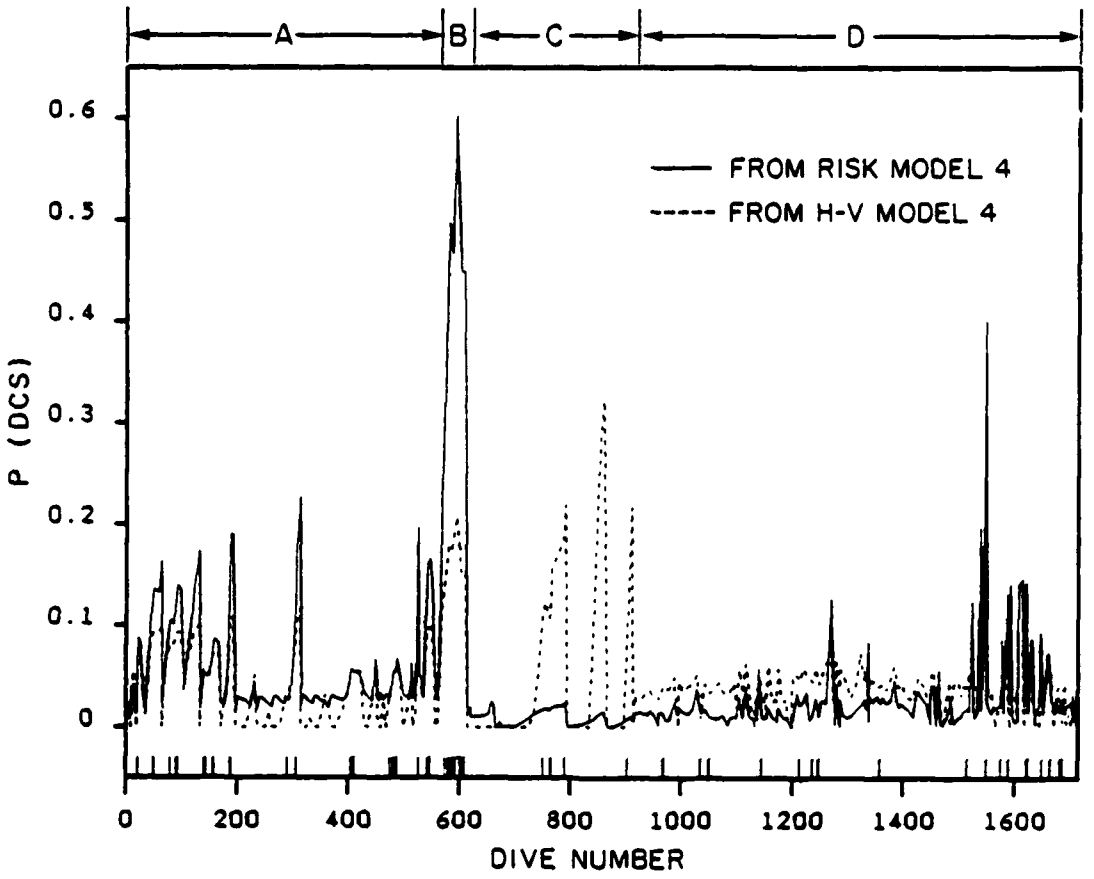

Figure 8

Comparison of risk model and H-V Model for Data Det ABCD

Data (Dive Number)	bend%	average P(DCS) by R4	average P(DCS) by H-V4
A (1--568)	4.8%	5.6%	3.9%
B (569--614)	45.6%	43.4%	16.3%
C (615--913)	1.3%	.8%	4.6%
D (914--1713)	3.0%	2.8%	4.0%

*bar below 0 indicates incidence of bends

TABLE 9

(DATA SET ABD, N = 1414, BENDS = 72)

MODEL (FIXED PARAMETERS)	PARAMETERS (1 SE)		LOG LIKELIHOOD
0. CONSTANT P	P = 0.051		-284.516
1. NT = 1, POWER = 1,	D50 = 2.42	(0.35)	-237.498
	T = 370	(90)	
	CR = 1.0000	(0.047)	
2. NT = 1,	POWER = 2.45	(0.55)	-224.901
	D50 = 0.69	(0.08)	
	T = 309	(29)	
	CR = 1.00000	(0.04)	
3. NT = 2, POWER = 1	D50 = 2.45	(0.42)	-237.345
	T1 = 466	(755)	
	CR1 = 1.00000	(0.29)	
	T2 = 368	(119)	
	CR2 = 1.00000	(0.06)	
4. NT = 2,	POWER = 2.48	(0.52)	-224.073
	D50 = 0.68	(0.08)	
	T1 = 318	(35)	
	CR1 = 1.00000	(0.04)	
	T2 = 135	(66)	
	CR2 = 1.29	(0.19)	
Q1. NT = 1, POWER = 1,			same as 1
Q2. NT = 1			same as 2
R4. 2-tissue, thresh	TA = 17.6	(22)	-221.415
	AA = 1.13E-3	(1.05E-3)	
	TB = 258	(41)	
	AB = 8.10E-3	(3.5E-3)	
	PTHR = 5.3	(1.9)(fsw)	

T, T1, etc. are in units of minutes, the other parameters are dimensionless.

Approximate 1 SE error limits on estimated parameters are in parentheses.

Expected LL for excellent fit = -207.

H-V models than for the risk models. All successful models in Table 9 still fall short of the combined single set good LL of -90-22-95 = -207.

9. DATA SET L: SATURATION DIVES

The final data set examined was used only in Report IV (5). It consists of 122 exposures on 14 different air saturation exposures where the divers were at constant increased pressure for at least 40 hours before decompression. In Report IV (5), a larger data set was examined that had N_2-O_2 mixtures other than air, but they are excluded here to keep all data for air exposures only. Model performance is in Table 10. Only a single long (over 700 min) time constant is required, and the likelihood of Model 1 is not actually significantly better than the null model (Model 0) by formal likelihood ratio tests. The POWER in Model 2 is not higher than 1 by a significant amount. The risk model listed performs comparably, but is not a significant improvement over the null model. By itself, the data set is too small to support any useful modeling with any of the methods tried. For the rough expected LL of combined sets, we will carry an LL of about -58 for set L.

10. DATA SET ABCDL

The final set of fits is for all of the data combined: 1,835 different dives. Table 11 shows that both two- and three-tissue H-V models were a great improvement over the null model. The significant improvement by the three-tissue model requires a time constant of over 1000 min. For both of the longer time constants, no supersaturation is perfectly safe (CR essentially 1.0). The POWER is not much different from 1. The risk models again do much better than H-V models.

The best H-V model (Model 5) and a successful risk model (R8) are both shown in Fig. 9. R8 is also much better than the H-V model in the combination of all 5 data sets by the likelihood criteria since it misses the target LL by

TABLE 11

(DATA SET ABCDL, N = 1835, BENDS = 100.5)

MODEL (FIXED PARAMETERS)	PARAMETERS (1 SE)		LOG LIKELIHOOD
0. CONSTANT P	P = 0.054768		-389.613
1. NT = 1, POWER = 1			NA
2. NT = 1			NA
3. NT = 2, POWER = 1	D50 = 2.25	(0.27)	-338.430
	T1 = 0.93	(0.09)	
	CR1= 4.54	(0.04)	
	T2 = 379	(22)	
	CR2 = 1.00000	(0.009)	
4. NT = 2,			same as 3
5. NT = 3, POWER = 1	D50 = 2.64	(0.37)	-325.920
	T1 = 0.92	(0.10)	
	CR1 = 4.53	(0.05)	
	T2 = 363	(98)	
	CR2 = 1.00000	(0.05)	
	T3 = 1001	(619)	
	CR3 = 1.00000	(0.21)	
6. NT = 3	POWER = 1.19	(0.26)	-324.703
	D50 = 1.88	(0.65)	
	T1 = 0.92	(0.09)	
	CR1 = 4.52	(0.06)	
	T2 = 355	(91)	
	CR2 = 1.00001	(0.05)	
	T3 = 1038	(350)	
	CR3 = 1.00000	(0.0003)	
Q3. NT = 2, POWER = 1			same as 3
Q4. NT = 2			same as 3
R3. 2-tissue, no thresh	TA = 3.25	(1.77)	-308.575
	AA = 2.91E-3	(1.54E-3)	
	TB = 421	(22.1)	
	AB = 2.91E-3	(.353E-3)	
R8. 3-tissue, thresh	TA = 5.92	(1.96)	-302.779
	AA = 3.1E-3	(1.26E-3)	
	TB = 260	(39.4)	
	AB = 6.34E-3	(2.62E-3)	
	TC = 808	(176)	
	AC = 1.51E-3	(.944E-3)	
	PTHR = 4.67	(1.65)(fsw)	

TABLE 11 (Cont'd)

(DATA SET ABCDL, N = 1835, BENDS = 100.5)

MODEL (FIXED PARAMETERS)	PARAMETERS (1 SE)		LOG LIKELIHOOD
R9. 2-tissue each with 2-exp rtf no thresh	T1A = 1.77	(2.51)	-303.658
	T2A = 283	(40.9)	
	W1A = 0.988	(.000223)	
	AA = 8.29E-3	(2.9E-3)	
	T1B = 82.6	(123)	
	T2B = 891	(285)	
	W1B = 0.886	(0.011)	
	AB = 2.04E-3	(2.52E-3)	
R10. 2-tissue each with 2-exp rtf thresh			same as R9

T, T1, etc. are in units of minutes, the other parameters are dimensionless.

Approximate 1 SE error limits on estimated parameters are in parentheses.

Expected LL for excellent fit = -283.

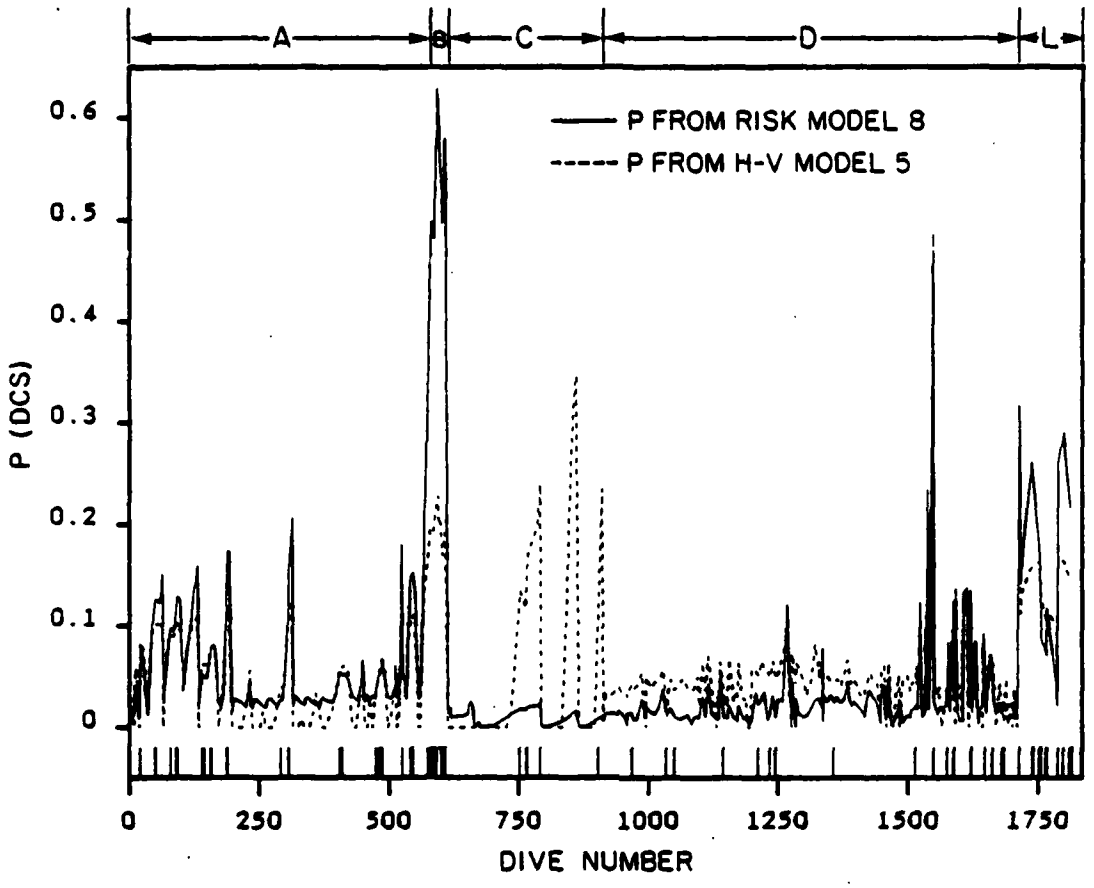

Figure 9

Comparison of Risk Model and H-V Model for Data Set ABCDL

Data (Dive Number)	bend%	average P(DCS) by R8	average P(DCS) by H-V5
A (1--568)	4.8%	5.3%	4.2%
B (569--614)	45.6%	46.4%	18.3%
C (615--913)	1.3%	.8%	5.0%
D (914--1713)	3.0%	2.9%	4.4%
L (1714--1835)	20.1%	19.1%	14.2%

*bar below 0 indicates incidence of bends

about 20 units instead of over 40 units. Failure to fit component data is apparent in a similar manner to that seen in previous combined data (Figs. 5 and 8). This reinforces our conclusion that H-V decompression response function is not suitable for different data.

VI. CONCLUSION

In general, Haldane-Vann models with a single tissue are adequate for small data sets of roughly similar dives. When combined with dissimilar dives, the fits degrade as first noted by Vann (6). Specifically, the gas exchange kinetics apparently can adequately describe the different dives, but a single dose-response function causes problems. Even the allowance of a separate critical ratio for each time constant does not suffice. Perhaps the use of separate D50 and POWER parameters for each tissue would produce more reasonable descriptions of the combined data, but the need for 4 or 5 parameters per tissue would be difficult to justify statistically. The risk model aspect of integrating a supersaturation over its elapsed time appears to capture essential aspects of decompression outcome substantially better than the choice of a maximum "stress" as used in the H-V approach.

VII. REFERENCES

1. Weathersby, P.K., L.D. Homer, and E.T. Flynn. "On the likelihood of decompression sickness." Journal of Applied Physiology, Vol. 57 pp. 815-825, 1984.

2. Weathersby, P.K., S.S. Survanshi, L.D. Homer, B.L. Hart, E.T. Flynn, and M.E. Bradley, Statistically based decompression tables I. Analysis of standard air dives: 1950-1970, NMRI 85-16, Naval Medical Research Institute, Bethesda, MD, March 1985a.

3. Weathersby, P.K., J.R. Hays, S.S. Survanshi, L.D. Homer, B.L. Hart, E.T. Flynn, and M.E. Bradley, Statistically based decompression tables II. Equal risk air diving decompression schedules, NMRI 85-17, Naval Medical Research Institute, Bethesda, MD, March 1985b.

4. Weathersby, P.K., S.S. Survanshi, J.R. Hays, and M.E. MacCallum, Statistically based decompression tables. III. Comparative risk using U.S. Navy, British, and Canadian standard air schedules, NMRI 86-50, Naval Medical Research Institute, Bethesda, MD, July 1986a.

5. Hays, J.R., B.L. Hart, P.K. Weathersby, S.S. Survanshi, L.D. Homer, and E.T. Flynn. Statistically based decompression tables IV. Extension to air and N2-O2 decompression, NMRI 86-51, Naval Medical Research Institute, Bethesda, MD, July 1986.

6. Vann, R.D., A likelihood analysis of decompression data using Haldane and bubble growth models, Proceedings of the Ninth International Symposium on Underwater and Hyperbaric Physiology, Undersea and Hyperbaric Medical Society, Bethesda, MD, pp. 165-181, 1987.

7. Boycott, A.E., G.C.C. Damant, and J.S. Haldane, "The prevention of compressed air illness." Journal of Hygiene (Cambridge), Vol. 8, pp. 342-443, 1908.

8. Weathersby, P.K., B.L. Hart, E.T. Flynn, and W.F. Walker, Human decompression trial in nitrogen-oxygen diving, NMRI 86-97, Naval Medical Research Institute, Bethesda, MD, August 1986b.

9. Des Granges, M., Standard air decompression table, EDU-TR-5-57, U.S. Navy Experimental Diving Unit, Panama City, FL, December 1956.

10. Workman, R.D., Calculation of air saturation decompression tables, EDU-TR-11-57, U.S. Navy Experimental Diving Unit, Panama City, FL, June 1957.

11. Donald, K.W., A review of submarine escape trials from 1945-1970 with particular emphasis on decompression sickness. Medical Research Council Underwater physiology Report No. 290. London: Her Majesty's Stationers Office; 1970.

12. Tikuisis P., R.Y. Nishi, and P.K. Weathersby, Use of the maximum likelihood method in the analysis of chamber air dives, Undersea Biomedical Research, Vol. 15, pp. 301-313, 1988.

13. Kendall, M.G. and A. Stuart. The advanced theory of statistics, 4th ed, Vol. 2, Haffner Publishing Co., London, England, 1979.

14. Marquardt, D.W., "An algorithm for least-squares estimation of nonlinear parameters." Journal of the Society for Industrial and Applied Mathematics, Vol. 11, No. 2, pp. 431-441, June 1963.

15. Bailey, R.C. and L.D. Homer, An analogy permitting maximum likelihood estimation by a simple modification of general least squares algorithms, NMRI 77-55. Naval Medical Research Institute, Bethesda, MD, 1977.

16. Workman, R.D., Calculation of decompression schedules for N2-O2 and He-O2 dives, EDU-TR-6-65, U.S. Navy Experimental Diving Unit, Panama City, FL, May 1965.

17. Diem, K., editor. Documenta Geigy Scientific Tables. Sixth Edition. Ardsley, NY: Geigy Chem. Corp.; 1962: 85-106.

18. Weathersby, P.K. E.E.P. Barnard, L.D. Homer, and K.G. Mendenhall. Stochastic description of inert gas exchange. Journal of Applied Physiology: Respiratory, Environmental and Exercise Physiology, Vol. 47, pp. 1263-1269, 1979.

19. Weathersby, P.K., K.G. Mendenhall, E.E.P. Barnard, L.D. Homer, S. Survanshi, and F. Vieras. The distribution of xenon gas exchange rates in dogs. Journal of Applied Physiology: Respiratory, Environmental and Exercise Physiology, Vol. 50, pp 1325-1336, 1981.

APPENDIX A: RISK MODEL SUMMARY

The risk models are described in more detail in Reports I and IV (2,5), but are summarized below. All definitions of r are substituted into Eqn. [1] to calculate a P(DCS) for each dive.

Model R1: $r1 = A (Ptis - Pamb) / Pamb$ [2]

Ptis by monexponential; time constant = T

2 parameters: A, T

Ptis, a tissue inert gas partial pressure calculated by treating the tissue as a single, well-mixed compartment, is compared to Pamb, the current ambient pressure. As is common in decompression calculations, the metabolic gases O_2 and CO_2 and water vapor are totally ignored. Whenever Ptis is less than Pamb, R1 is set to zero. The risk R1 is proportional to the supersaturation with a proportionality parameter A in units of min^{-1} (T in min). The appearance of Pamb in the denominator follows from previous work with deep saturation-excursion data (1) in which it was shown that a significant decrease in DCS occurred if an equal supersaturation was created at deeper depths. The next model adds a threshold parameter, PTHR, that allows the possibility that a supersaturation can be sustained indefinitely without risk of DCS:

Model R2: $r2 = A (Ptis - Pamb - PTHR) / Pamb$ [3]

Ptis by monexponential; time constant = T

3 parameters: A, T, PTHR

PTHR is a constant parameter independent of depth. Again, only positive values of the numerator will be allowed in the integration of Eqn. 1. Model R1 can be generalized to include a "second tissue" that has its own time

constant and proportionality parameter. The statistical sense of this model is that no DCS is the joint probability of no DCS in both tissue. No anatomic identification of the second (or indeed the first) tissue is attempted. This model is expressed by:

Model R3: r3 = r3A + r3B, where [4]

r3A = AA (PtisA - Pamb) / Pamb

PtisA by monoexponential; time constant = TA

r3B = AB (PtisB - Pamb) / Pamb

PtisB by monoexponential; time constant = TB

4 parameters: AA, TA, AB, TB

This "two tissue" model can also have an added threshold parameter:

Model R4: r4 = r4A + r4B, where [5]

r4A = AA (PtisA - Pamb - PTHR) / Pamb

PtisA by monoexponential; time constant = TA

r4B = AB (PtisB - Pamb - PTHR) / Pamb

PtisB by monoexponential; time constant = TB

5 parameters: AA, TA, AB, TB, PTHR

An alternative to the "two-tissue" model is one in which more complex gas exchange kinetics are utilized. The gas residence time function (rtf) (18,19) is an empirical multi-exponential description of gas exchange in a single tissue that has three kinetic parameters, one of which being a weighting constant, rather than the one kinetic parameter of a single exponential. This model is described by:

Model R5: r5 = A (Ptis - Pamb) / Pamb [6]

Ptis by 2 exponentials; time constants = T1 and T2

Fraction of rtf by T1 is W1;

Fraction of rtf by T2 is 1 - W1;

4 parameters: A, T1, T2, W1

This model performed well on the more than 1,700 air decompression dives in the Report I (2), and was used in the calculation of the new air decompression tables in Report II (3).

To parallel the previous developments, a threshold parameter can also be defined for the two exponential exchange model:

Model R6: r6 = A (Ptis - Pamb - PTHR) / Pamb [7]

Ptis by 2 exponentials; time constants = T1 and T2

Fraction of rtf by T1 is W1;

Fraction of rtf by T2 is 1 - W1;

5 parameters: A, T1, T2, W1, PTHR

A new model was needed to describe the combination of the short air decompression and saturation data. Models R7-R10 were developed for this purpose. Four new models were developed in a fashion similar to the development of the first 6 models. Model 3 was extended to include "three tissues" rather than the "two tissues" as previously described. No DCS is the the joint probability of no DCS in all three tissues. The new model is expressed by:

Model R9: r9 = r9A + r9B, where [10]

r9A = AA (PtisA - Pamb) / Pamb

PtisA by 2 exponentials; time constants = T1A and T2A

Fraction of rtf by T1A is W1A;

Fraction of rtf by T2A is 1 - W1A;

r9B = AB (Ptis - Pamb) / Pamb

PtisB by 2 exponentials; time constants = T1B and T2B

Fraction of rtf by T1B is W1B;

Fraction of rtf by T2B is 1 - W1B;

8 parameters: AA, T1A, T2A, W1A, AB, T1B, T2B, W1B

Adding a threshold parameter yields:

Model R10: r10 = r10A + r10B, where [11]

r10A = AB (PtisA - Pamb - PTHR) / Pamb

PtisA by 2 exponentials; time constants = T1A and T2A

Fraction of rtf by T1A is W1A;

Fraction of rtf by T2A is 1 - W1A;

r10B = AB (PtisB - Pamb - PTHR) / Pamb

PtisB by 2 exponentials; time constants = T1B and T2B

Fraction of rtf by T1B is W1A + W1B;

Fraction of rtf by T2B is 1 - W1B;

9 parameters: AA, T1A, T2A, W1A, AB, T1B, T2B, W1B, PTHR

APPENDIX B: MATHEMATICAL ASPECTS OF HALDANE-VANN MODELS

In a dive for which the plot of depth vs. time consists of a series of line segments (ramp) connected at "nodes", when does the maximum ratio of inert gas pressure in the tissue to ambient pressure occur in a ramp? The following Lemma will show that, under certain assumptions, for a curve f(t) and a line segment g(t), the maximum of the ratio f(t)/g(t) occurs at one of the nodes of the ramp. This lemma will be used in the algorithm for finding the maximum ratio in certain kinds of situations, which will be presented thereafter.

Lemma

For $t1 \le t \le t2$, $f(t) > 0$, $g(t) > 0$, $g(t)$ is a line.

fc(t) = chord of f = line segment from (t1,f(t1)) to (t2,f(t2))

If $f(t) \le fc(t)$, then

$\max\{ f(t)/g(t): t1 \le t \le t2 \} = \max\{ f(t1)/g(t1), f(t2)/g(t2) \}$.

proof:

Let $f1 = f(t1)$, $f2 = f(t2)$,

$g1 = g(t1)$, $g2 = g(t2)$,

$m1 = f1/g1$, $m2 = f2/g2$.

Thus $g(t) = g1 + (t - t1)\ (g2-g1)/\ (t2-t1)$,

$fc(t) = f1 + (t - t1)\ (f2-f1)/\ (t2-t1)$.

Suppose $m1 \ge m2$, $m1g2 \ge m2g2 = f2$,

then $m1 \cdot g(t) = m1g1 + (t - t1)\ (m1g2-m1g1)/\ (t2-t1)$

$\ge m1g1 + (t - t1)\ (m2g2-m1g1)/\ (t2-t1)$

$= f1 + (t - t1)\ (f2-f1)/\ (t2-t1)$

$= fc(t) \ge f(t)$ (by assumption).

therefore $f(t) \le m1 \cdot g(t)$, $f(t)/\ g(t) \le m1$.

Similarily, if m1 < m2 then $f(t)/g(t) \leq m2$.

So $\max\{ f(t)/g(t) : t1 \leq t \leq t2 \} = \max\{ f(t1)/g(t1), f(t2)/g(t2) \}$

(end of proof)

Now to apply the lemma:

Let f(t) = PT(t) = Pressure of inert gas in tissue at time t,

g(t) = PN(t) = External pressure of inert gas at time t,

PA(t) = g(t)/0.79 = Total ambient pressure (hydrostatic pressure) at time t,

CR(t) = critical ratio = $r - sc \cdot (PA(t))$, $r \geq 1$, $sc \geq 0$.

From Report I, between two nodes, $0 \leq t \leq t2$,

$f(t) = d - a\,b + b\,t + c \exp(-t/a) > 0$, $a > 0$

for monoexponential gas exchange kinetics.

$g(t) = d + b\,t > 0$,

then $f(t)/g(t) = 1 + [-a\,b + c \exp(-t/a)]/g(t)$.

Define $DR(t) = [PT(t) / PA(t)] - CR(t)$

$DR(t) = 0.79\, f(t)/g(t) - r + sc\, g(t) /0.79$

$= -r + 0.79\{1 + [-a\,b + c \exp(-t/a)]/g(t) + sc\, g(t)/(0.79^2)\}$

Let $s = sc/(0.79^2)$ (so $s > 0$) and

$R(t) = [-a\,b + c \exp(-t/a)]/g(t) + s\, g(t)$

then $DR(t) = -r + 0.79\,\{1 + R(t)\}$.

IF $f(t)/g(t) < 1$ ($[-a\,b + c \exp(-t/a)] < 0$), the risk consequently is zero, making calculation of the ratio unnecessary.

For $b>0$ and $c<0$, $f(t)/g(t) \leq 1$ for all t in $[0,t2]$

For $b>0$ and $c>0$, $f(t)/g(t) \leq 1$ if $t \geq a \ln(c/(a\,b))$.

For $b<0$ and $c<0$, $f(t)/g(t) \leq 1$ if $t \leq a \ln(c/(a\,b))$.

Now the goal is to find

max {R(t), where t in [0,t2] and f(t)/g(t) > 1}

(I) If b = 0, (no depth change)

finding max R(t) is equivalent to finding max {c exp(-t/a)}. Since this function is monotone, max R(t) is at one of the end points.

(II) If s = 0, (constant critical ratio)

finding max R(t) is equivalent to finding max f(t)/g(t).

(II.1) If s = 0, c >= 0, max f(t)/g(t) is at one of the end points.

proof:

If c = 0, then f(t) = fc(t).

If c > 0, then $f''(t) = c \exp(-t/a)/(a^2) > 0$. Therefore, f is concave upward and f(t) <= fc(t) (Stein: Calculus and Analytical Geometry, p. 188).

By Lemma, max f(t)/g(t) is at one of the end points.

(II.2) If s = 0, c < 0, b < 0, max f(t)/g(t) = f(t2)/g(t2).

proof:

$f(t)/g(t) = 1 + [-a\ b + c \exp(-t/a)] \ / \ (d+bt)$

Since [-a b + c exp(-t/a)] increases with t and (d+bt) decreases with t, then f(t)/g(t) must increase with t and be a maximum at t2.

(III) s > 0: (variable critical ratio)

(III.1) If s > 0, c $\geq$ 0, max R(t) is at one of the end points.

proof:

$[\text{numerator of } R(t)]'' = 2b^2s + c \exp(-t/a) \ / \ (a^2) > 0;$

therefore, [numerator of R(t)] is concave upward and is $\leq$ its chord(Stein: Calculus and Analytical Geometry, p. 188).

By Lemma, max R(t) is at an end point.

(III.2) If s > 0, c < 0, b < 0 , we can't tell the behavior of R(t),

need to solve $R'(t)=0$ in order to find max $R(t)$.

$R'(t)=[sb\ g(t)^2 + a\ b^2 - c(g(t)/a + b)\ \exp(-t/a)]/\ (g(t)^2)$

Let $Q(t)=$ [numerator of $R'(t)$].

Now solve for $Q(t) = 0$. Where is $Q(t)$ increasing?

$Q(t)$ increasing (i.e., $Q'(t) = g(t)\ [2sb^2 + c\ \exp(-t/a)\ /\ (a^2)] \geq 0$)

if and only if $t \geq a\ \ln(-c/2a^2b^2s)$.

Let $tag = a\ \ln(-c/2a^2b^2s)$.

Case 1: $t \geq tag$ (if $tag \leq t \leq t2$).

$Q(t)$ increases with t.

Since $g(t) > 0$ and decreasing, $g(t)^2$ also decreases with t.

So $R'(t)$ increases with t, $R(t)$ is concave upward.

$\max\{ R(t),\ tag \leq t \leq t2 \} = \max\ \{ R(tag),\ R(t2) \}$

Case 2: $t < tag$ (if $0 \leq t < tag \leq t2$ or $0 \leq t \leq t2 < tag$).

Let $top = \min\{tag, t2\}$.

$Q(t)$ strictly decreases with t, where $0 \leq t < top$

If $Q(0) \leq 0$, then $Q(t) \leq 0$, $R'(t) \leq 0$ and $R(t)$ decreasing,

$\max\{ R(t),\ 0 \leq t \leq top \} = R(0)$.

If $Q(top) \geq 0$, then $Q(t) \geq 0$, $R'(t) \geq 0$ and $R(t)$ increasing,

$\max\{ R(t),\ 0 \leq t \leq top \} = R(top)$.

If $Q(0) > 0$ and $Q(top) < 0$ then there is only one root for

$Q(t) = 0$ in $[0, top]$, say $Q(tr) = 0$.

For $0 \leq t \leq tr$, $Q(t) \geq 0$, $R'(t) \geq 0$, $\max R(t) = R(tr)$.

For $tr \leq t \leq top$, $Q(t) \leq 0$, $R'(t) \leq 0$, $\max R(t) = R(tr)$.

APPENDIX C: GRAPHICAL REPRESENTATION OF GOODNESS-OF-FIT

When data consist of two variables such as temperature taken at different times, it is easy to plot the time/temperature pairs and the model function simultaneously and look for points far from the model curve. In the case presented in this report that easy plot is unavailable. Instead of a single independent variable like time, diving data consist of many pressure/time points for each observation, and therefore do not form a useful abscissa for plotting. The ordinate variable is not much easier. The predicted ordinate would be P(DCS), but the raw data are a 0 or a 1 at each point. (If we had enough, for example, 50-100 replicate dives at each dive profile, an average bend % would be valuable. But this is not the case in our data).

Figure C-1 is similar to plots used in Report I (2) where the dives are broken into categories depending on the model's estimate of DCS risk in the dive. Fits of model to Data Set A are used in the plot. Here four categories are used: safer than 2% P(DCS), 2-5%, 5-10%, and over 10% P(DCS). For example 132 exposures were predicted to fall in the range of 5-10% DCS; the average prediction was 7.6%, and about 95% of the predictions were in the range of 6.73-8.75%. On the actual dives, some 11 cases of DCS were observed, for a raw incidence of 8.3%. Reference to binomial distribution with N=132 and p= 8.3% gives 95% confidence limits of 4.2-14.4% on the raw outcome (13,17). In Fig. C-1 are plotted the average predicted and observed incidence of DCS for the 4 categories of risk (shown as stars). "Perfect" fitting would presumably give us points on the dotted line of observed = predicted. However, uncertainty in both predictions and observations allow non-significant deviations from the line of identity. In Fig. C-1, the rectangles show the extent of 95% of both predictions (rectangle width) and observations (rectangle height) for each of the four categories.

The dotted line clearly passes through each rectangle. Note that the large size of rectangle makes "agreement" between observation and prediction rather easy. By Pearson's goodness-of-fit test (13) the conclusion from Fig. C-1 is that P(DCS) agrees well with prediction for all categories.

Another way to visualize success in predicting individual dives is shown in Fig. C-2. All dives were ranked from safest to most hazardous by predicted P(DCS). A point on the solid line corresponding to a certain value of P(DCS) is the sum of P(DCS) for all dives of that value or safer (For example all 342 dives of P(DCS) of 6.5% or safer totalled 3.7 cases predicted). A horizontal line means that no dives were conducted with P(DCS) in that range. At each prediction where a case of DCS was observed to occur, a triangle records the cumulative number of cases. A "perfect" fit will have the line increase near where the triangles appear. However, both data triangles and the prediction line do not plot independent features: both have accumulated aspects of all points to the left. Even the null model will result in agreement: it will appear as a single vertical line at the average p(DCS) and all triangles will fall on the line. For other poorly fitting models, agreement at the final point where overall average incidence equals overall average outcome also frequently occurs. Agreement at intermediate points will tend to be achieved by the triangles crossing back and forth across the line as if predictions "compensate" for earlier disagreements. Thus the plot has minimal value for diagnosing problems in the fit.

Both graphical approaches have such little power to provide useful goodness-of-fit information that we will not use this presentation for other data.

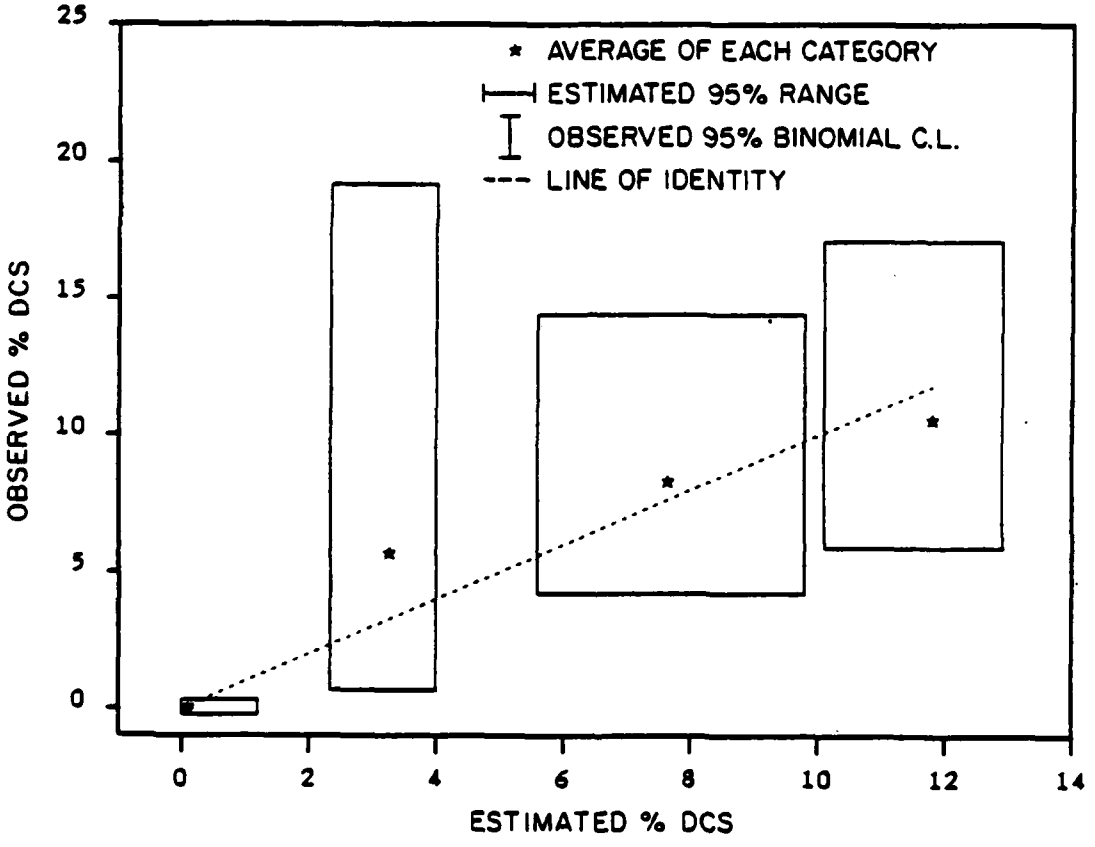

Figure C-1

Observed vs. Estimated Incidence for Data Set A

Data Set A, Model 1. Estimated P(DCS) are divided into 4 categories: 0-2%, 2-5%, 5-10%, and 10-100%.

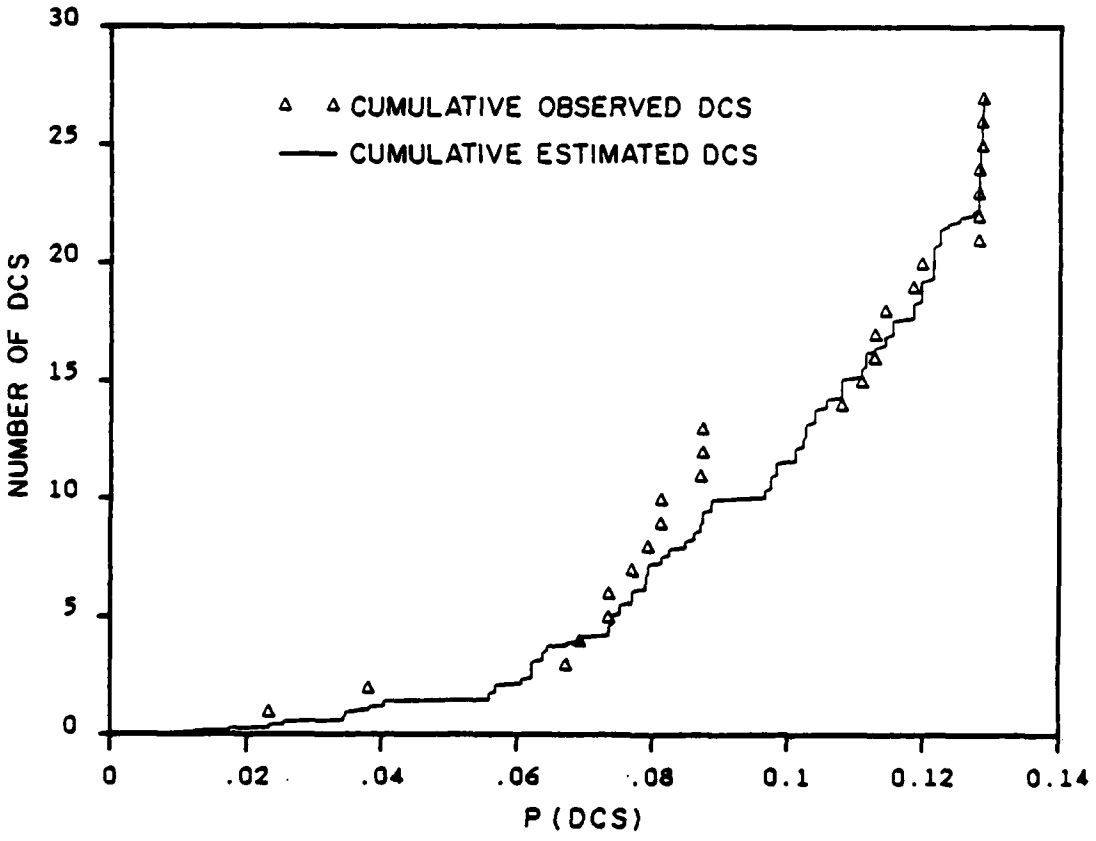

Figure C-2

Observed vs. Estimated DCS for Data Set A

Data Set A, Model 1.

END

FILMED

1-90

DTIC